Welding in the World (2023) 67:1997–2005
https://doi.org/10.1007/s40194-023-01533-3

RESEARCH PAPER

# Study on joint characteristics in laser butt welding of AMed and wrought Ti6Al4V plates

Yasuhiro Okamoto[1] · Togo Shinonaga[1] · Yoshito Takemoto[1] · Akira Okada[1] · Akihiro Ochi[1] · Ryuya Kishimoto[1] · Sisa Pityana[2] · Nana Arthur[2] · Peter Omoniyi[3,4] · Rasheedat Mahamood[3,4] · Martin Maina[5] · Esther Akinlabi[3,6,7]

Received: 11 August 2022 / Accepted: 9 May 2023 / Published online: 8 June 2023


## Abstract

Titanium alloy Ti6Al4V has been widely applied to medical, automotive, and aerospace industries due to its excellent properties such as high strength and excellent corrosion resistance. On the other hand, additive manufacturing (AM) technology can give the freedom of design of the products. In order to spread the AMed products, the joining of AMed and wrought products are required, and it is important to understand the joint characteristics. In this study, butt welding of Ti6Al4V plate was conducted by fiber laser in argon shielding, and the joint characteristics of laser weld wrought/wrought, AMed/AMed, and AMed/wrought Ti6Al4V plates were experimentally investigated. The AMed plate has higher tensile strength than wrought plate but the elongation of AMed plate is smaller, since AMed plate has α' martensite due to rapid cooling during laser irradiation in AM process. Then, the laser weld joint of AMed/AMed plates has higher tensile strength, but smaller elongation than that of wrought/wrought plates. The weld joint of AMed/wrought plates shows good welding state, since small heat input leads to formation of small weld bead with higher hardness between wrought and AMed plates.

**Keywords** Ti6Al4V · Joint characteristics · Laser welding · Butt welding · Additive manufacturing

Recommended for publication by Commission IV - Power Beam Processes

✉ Togo Shinonaga
shinonaga@okayama-u.ac.jp

Yasuhiro Okamoto
Yasuhiro.Okamoto@okayama-u.ac.jp

Yoshito Takemoto
tanutake@okayama-u.ac.jp

Akira Okada
akira.okada@okayama-u.ac.jp

Akihiro Ochi
ochi_ntmlab@s.okayama-u.ac.jp

Ryuya Kishimoto
p8a20s83@s.okayama-u.ac.jp

Sisa Pityana
spityana@csir.co.za

Nana Arthur
NArthur@csir.co.za

Peter Omoniyi
omoniyi.po@unilorin.edu.ng

Rasheedat Mahamood
mahamoodmr2009@gmail.com

Martin Maina
mmaina@jkuat.ac.ke

Esther Akinlabi
etakinlabi@gmail.com

[1] Okayama University, Okayama, Japan

[2] National Laser Centre, CSIR, Pretoria, South Africa

[3] University of Johannesburg, Johannesburg, South Africa

[4] University of Ilorin, Ilorin, Nigeria

[5] Jomo Kenyatta University of Agriculture and Technology, Nairobi, Kenya

[6] Pan Africa University for Life and Earth Sciences Institute, Ibadan, Nigeria

[7] Northumbria University, Newcastle, UK

## 1 Introduction

Titanium alloy Ti6Al4V has been widely applied to biomaterials, automotive, and aerospace products due to its excellent properties such as high strength, low density, and excellent corrosion resistance. However, the Ti alloy is easily oxidized, since Ti alloy is well known as a highly active material. The mechanical properties of Ti alloy may reduce by the oxidization.

On the other hand, additive manufacturing (AM) technology can produce the products with complex shape, and the products can be freely designed by using 3D-CAD model data. Powder bed fusion (PBF) and directed energy deposition (DED) were commonly applied to produce the AMed metal products in the industrial field [1–3]. In general, AMed Ti6Al4V products are produced by PBF with an electron beam (electron beam melting: EBM) under vacuum ambience [4]. Recently, AMed Ti6Al4V products can be successfully produced by laser engineered net shaping technology (LENS), which belongs to DED technique with a laser beam [5, 6]. Large build volume can be obtained by LENS, compared with normal PBF process.

However, long processing time is needed for the creation of AMed metal products, and it is difficult to create the large products. In order to spread the AMed products, the joining of AMed and wrought products are required and it is important to understand the joint characteristics. The joint characteristics of AMed and wrought Ti6Al4V products have not been fully investigated yet. Then, laser welding can be applied to obtain low heat affected zone in shielding gas [7].

Therefore, in this study, laser welding of Ti6Al4V plates by fiber laser in argon shielding was proposed. As a fundamental study, laser butt welding of wrought/wrought, AMed/AMed, and AMed/wrought Ti6Al4V plates was conducted. Before laser butt welding, material characteristics such as crystal structure, microstructure, and mechanical properties of AMed and wrought Ti6Al4V plates were evaluated. Finally, laser weld joint characteristics of Ti6Al4V plates were experimentally investigated.

## 2 Experimental procedures

### 2.1 AMed and wrought Ti6Al4V plates

The AMed Ti6Al4V block with $110 \times 110 \times 40$ mm was produced by LENS technique with fiber laser beam. Schematic diagram of setup for LENS is shown in Fig. 1. AM conditions are shown in Table 1. The fiber laser beam with a spot diameter less than 1.4 mm and Gaussian mode was focused on the workpiece surface.

**Table 1** AM conditions

| | | | |
|---|---|---|---|
| Average laser power | $P_a$ | [W] | 400 |
| Spot diameter | $D_s$ | [mm] | 1.4 |
| Scanning speed | $V_s$ | [m/s] | 12.7 |
| Scan spacing | $D_p$ | [mm] | 0.97 |
| Layer thickness | $T_L$ | [mm] | 0.20 |
| Powder feed rate | $F_{pr}$ | [g/min] | 2.4 |

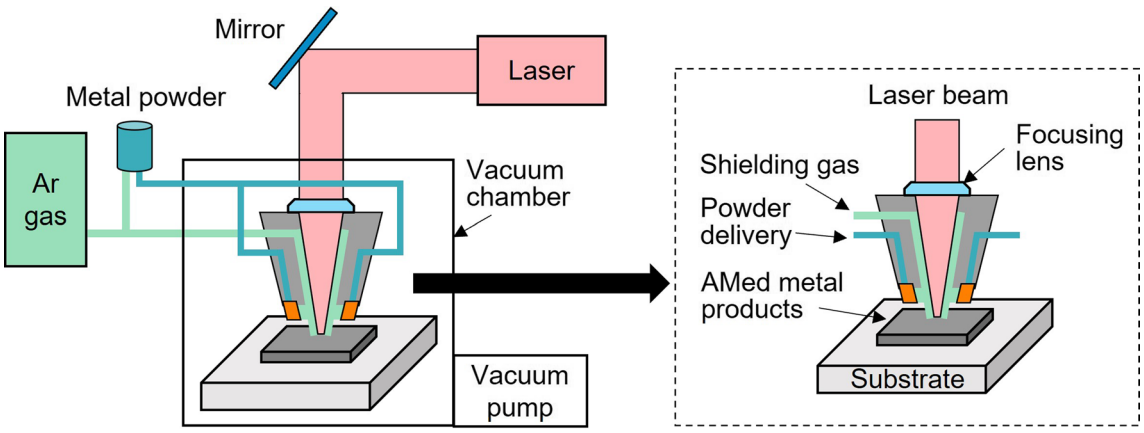


**Fig. 1** Schematic diagram of setup for LENS

**Table 2** Chemical compositions of Ti6Al4V powder (wt.%)

| Ti | Al | V | C | Fe |
|---|---|---|---|---|
| Val. | 6.44 | 4.06 | 0.01 | < 0.01 |
| N | O | H | Others | |
| 0.02 | 0.10 | 0.002 | Each < 0.10 | |

Average laser power was fixed to 400 W. The strategy of scanning path was cross hatch, and the scan spacing was fixed to 0.97 mm. A layer thickness was also fixed to 0.20 mm. Ti6Al4V powder with particle size between 40 and 100 μm was impacted to the workpiece surface, and the powder feed rate was about 2.4 g/min. Chemical composition of Ti6Al4V powder is shown in Table 2.

After building the Ti6Al4V block, the AMed block was slicing into 1 mm thickness by wire electrical discharge machine (EDM), and the AMed Ti6Al4V plates were obtained. The wrought Ti6Al4V plates with the same size as AMed ones were also prepared. In the welding experiment, the wrought and AMed Ti6Al4V without heat treatment were used, and electron back scattered diffraction (EBSD) image quality map and phase map of non-heated wrought specimen are shown in Fig. 2. α and β phases exist in the wrought plate as mentioned later, and the red and the green areas of phase map correspond to α phase and β one. According to the calculation of red and green areas, the ratio of β phase is 5.6%.

## 2.2 Laser butt welding

The joint characteristics of laser weld Ti6Al4V plates were experimentally investigated. Laser butt welding conditions are shown in Table 3. Schematic diagram of laser butt welding is shown in Fig. 3. Butt welding of wrought/wrought, AMed/AMed, and AMed/wrought Ti6Al4V plates with 1 mm thickness was conducted by fiber laser beam with double core in argon shielding. The laser irradiation conditions were determined for the best quality level for imperfections. Laser power of center part and ring part was 0.5 kW and 4.0 kW, respectively. The scanning velocity was 7.5 m/min. In order to suppress the oxidization of Ti6Al4V plates during laser welding, the argon gas was provided on top surface with flow rate of 15 L/min and the back surface with flow rate of 10 L/min.

## 2.3 Tensile test for laser weld plates

In order to conduct the tensile test of laser weld plate, the specimen was cut by wire EDM, and the size of specimen for tensile test was considerd according to the

**Table 3** Laser butt welding conditions

| | | | |
|---|---|---|---|
| Wavelength | $\lambda_a$ | [nm] | 1068–1080 |
| Thickness of plate | $t$ | [mm] | 1 |
| Laser power (center) | $P_c$ | [kW] | 0.5 |
| Laser power (ring) | $P_r$ | [kW] | 1.4 |
| Spot diameter (center) | $D_{sc}$ | [μm] | 150 |
| Spot diameter (ring) | $D_{sr}$ | [μm] | 600 |
| Scanning speed | $V_s$ | [m/min] | 7.5 |
| Angle of laser incident | $\theta_l$ | [°] | 10 |
| Ar shielding gas (top) | $F_{Art}$ | [L/min] | 15 |
| Ar shielding gas (back) | $F_{Arb}$ | [L/min] | 10 |

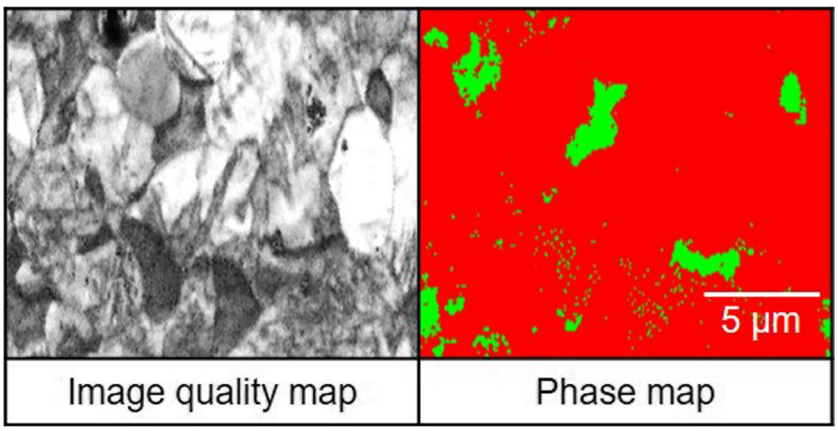


**Fig. 2** EBSD evaluation results of non-heated wrought Ti6Al4V

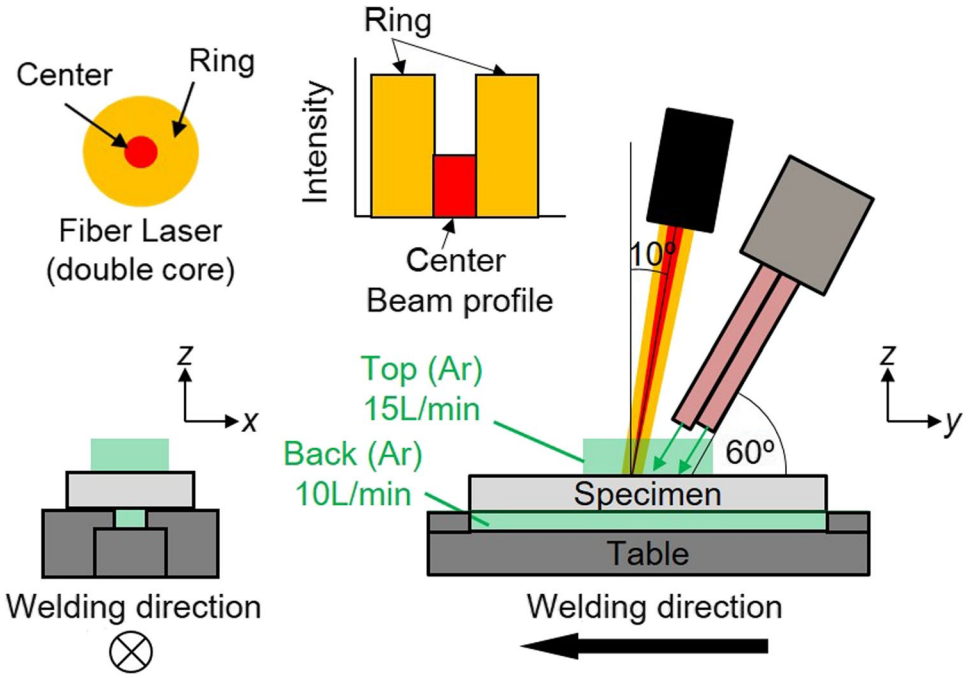


**Fig. 3** Schematic diagram of laser butt welding experiment

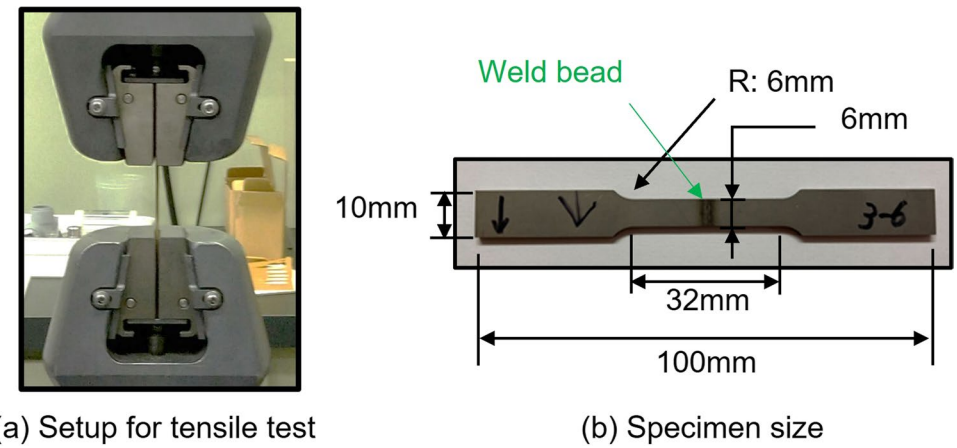


**Fig. 4** Schematic diagram of specimen for tensile test

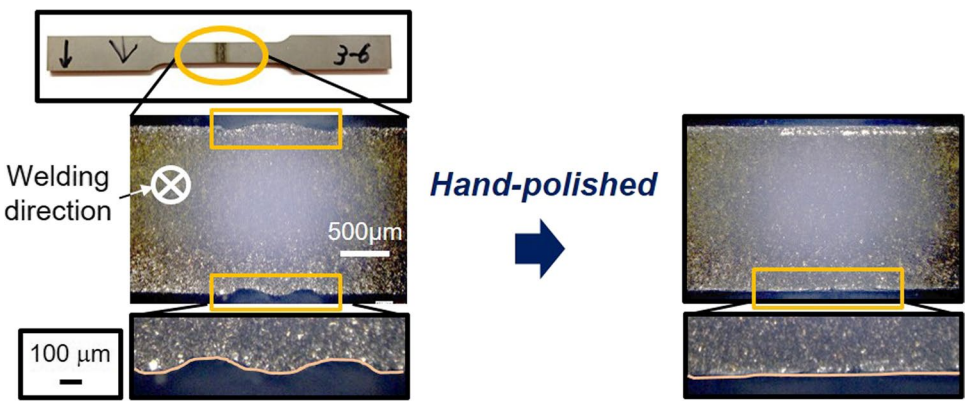


**Fig. 5** Polishing of laser weld specimen surfaces

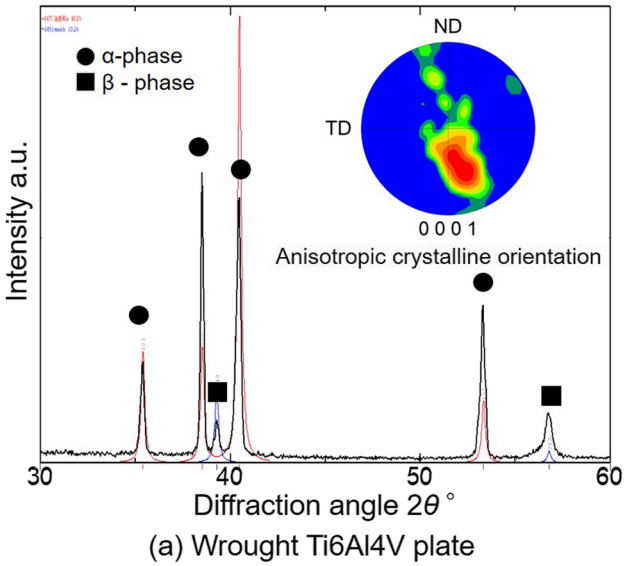


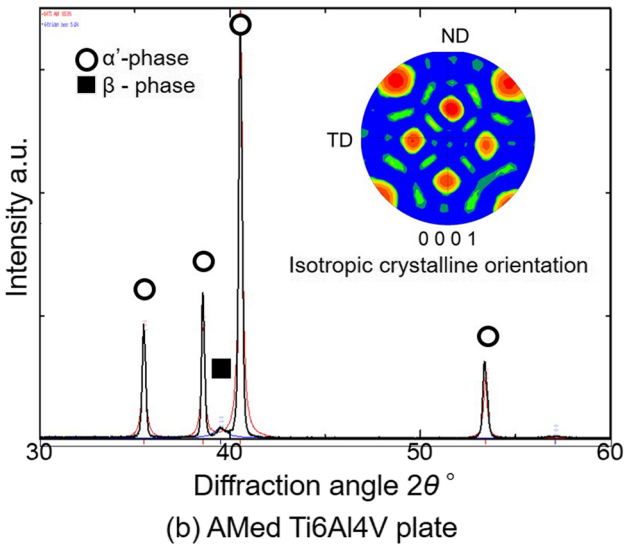


**Fig. 6** XRD patterns and pole figures of wrought and AMed Ti6Al4V plates

requirements of ASTM: E8 standards, as shown in Fig. 4. The equipment for tensile test is also shown in the figure. The crosshead speed for tensile test was set to 0.5 mm/min. Before the tensile test, the specimen surface was flat-polished in order to avoid the stress concentration at the weld bead as shown in Fig. 5.

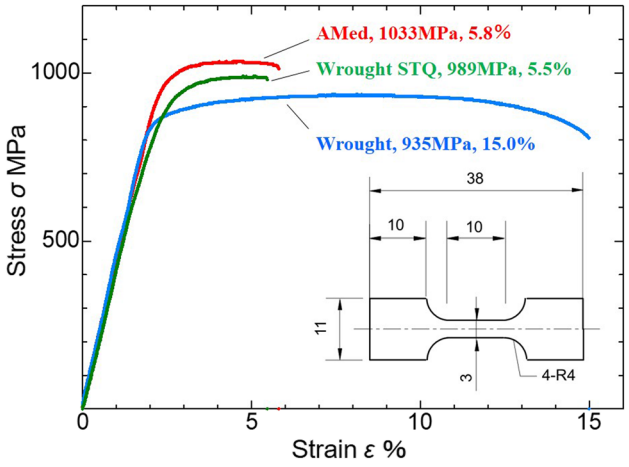


**Fig. 7** Stress–strain curves of AMed and wrought plates

## 3 Results and discussion

### 3.1 Characteristics of AMed and wrought Ti6Al4V plates

Before laser butt welding, the characteristics of AMed and wrought Ti6Al4V plates were investigated. Crystal structure of AMed and wrought plates was measured by X-ray diffraction (XRD). Crystalline orientation was also evaluated by pole figures, which were obtained from analysis of EBSD patterns. Figure 6 shows XRD patterns and crystalline orientation of wrought and AMed plates. The AMed plate consists of α' and β phases, while α and β phases exist in the wrought plate. The α' martensite would be generated by rapid cooling during laser irradiation, and it is known that α' martensite leads to high strength and brittle state of material. On the other hand, the AMed plate shows isotropic crystalline orientation, while anisotropic crystalline orientation is observed in the wrought plate by pole figures which were obtained from analysis of EBSD patterns.

Mechanical properties of AMed and wrought plates were measured. Figure 7 shows stress–strain curves of AMed and wrought plates. The curve of solution treated and quenched wrought plate (wrought STQ) is also shown in the figure. Quenching conditions of wrought

**Table 4** Young's modulus and Vickers hardness

| | | | | | |
|---|---|---|---|---|---|
| Young's modulus | AMed 110 GPa | ≒ | Wrought 111 GPa | ≒ | Wrought STQ 116 GPa |
| Vickers hardness | Wrought 321 HV | < | AMed 382 HV | < | Wrought STQ 404 HV |

STQ are heating at 1050 °C for 30 min under vacuum ambience. After heating, the wrought plate is cooling in ice-water, the cooling rate is about − 5000 °C/s. The wrought plate with heat treatment has crystal structure of α' and β phases, and anisotropic crystal orientation. As shown in the figure, the AMed plate had higher tensile strength than wrought plates with and without heat treatment, but the elongation of AMed plate is smaller than wrought plates without heat treatment. The wrought plate with heat treatment has small elongation similar to as AMed plate.

Table 4 shows Young's modulus and Vickers hardness of AMed and wrought Ti6Al4V plates with and without heat treatment. Young's modulus was measured by resonance method. AMed and wrought plates with and without heat treatment have similar Young's modulus of about 110 GPa. Hardness of AMed and wrought plates with heat treatment is higher than that of wrought without heat treatment.

The higher tensile strength and hardness of AMed plate are caused by microstructure of α' martensite. In addition, the isotropic crystalline orientation of AMed plate leads to higher tensile strength than the wrought plate with heat treatment. Meanwhile, limited elongation of AMed plate and wrought plate with heat treatment would be caused by microstructure of α'.

## 3.2 Joint characteristics in laser butt welding of Ti6Al4V plates

Figure 8 shows optical images of weld bead on the top and the back surfaces for wrought/wrought, AMed/AMed, and AMed/wrought Ti6Al4V plates 1 mm thick plates after laser butt welding. Non-heat treated specimens of AMed and wrought plates were used for laser welding. Similar weld bead appearance can be observed for all specimens. Oxidation can be suppressed on the top and the back surfaces by the argon gas shielding. These results indicate that good welding states can be obtained by laser butt welding for all the specimens.

Stress–strain curves for laser weld joint of AMed/AMed Ti6Al4V plates and the wrought/wrought ones were firstly compared. Tensile test was conducted three times in each specimen. Figure 9 shows stress–strain curves of laser weld joint of wrought/wrought, AMed/AMed, and AMed/wrought Ti6Al4V plates with 1 mm thickness. Fracture points and the fracture surface are also shown in the figure. Table 5 also shows average values of UTS, elongation, and fracture points of Fig. 9. All test pieces are not fractured on the weld bead but base material. The laser weld joint of AMed/AMed plates has the highest tensile strength, but the elongation is smaller than that of wrought/wrought plates. Then, brittle fracture state is observed at laser weld AMed/AMed plates, while ductile fracture is observed at laser weld wrought/wrought plates.

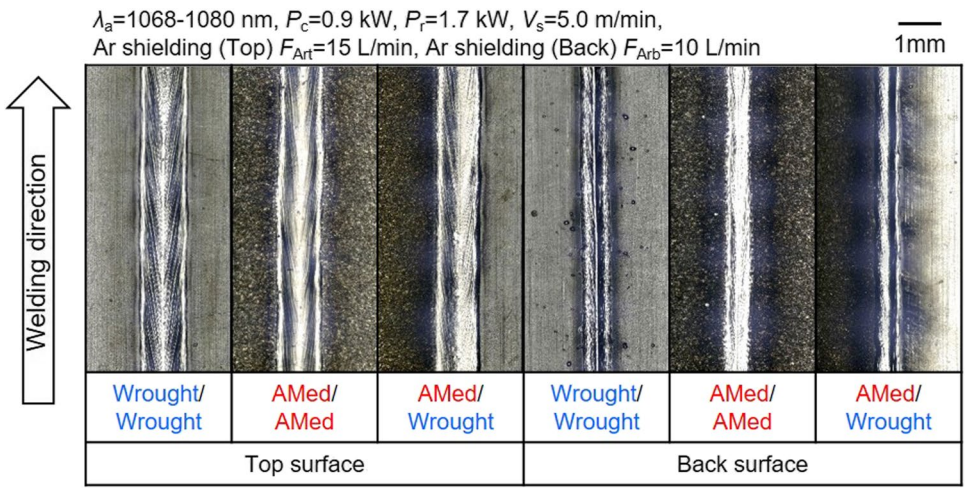


**Fig. 8** Optical images of weld bead on Ti6Al4V plates

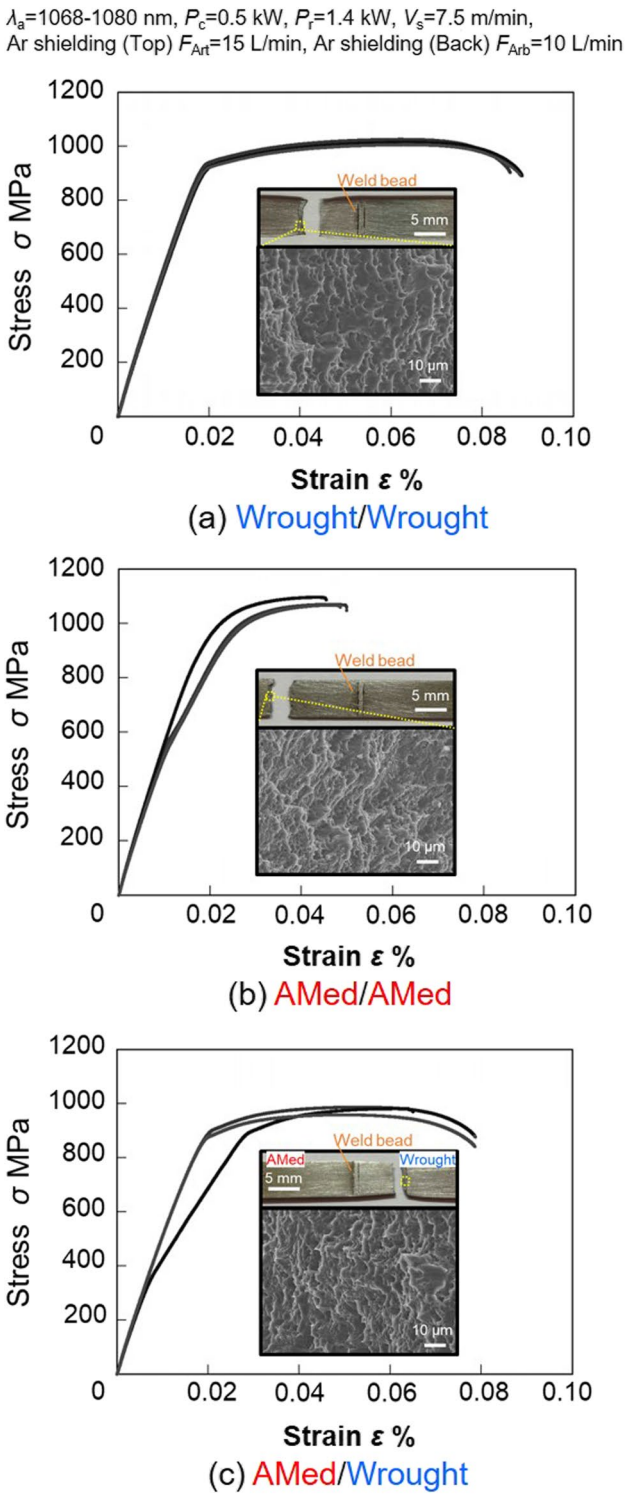


**Fig. 9** Stress–strain curves of laser weld joint of AMed/AMed, wrought/wrought, and AMed/wrought Ti6Al4V plates

**Table 5** Average values of UTS, elongation, and fracture point of Fig. 9

| | UTS [MPa] | Elongation [%] | Fracture point |
|---|---|---|---|
| Wrought/Wrought | 1016 | 0.088 | Wrought side |
| AMed/AMed | 1078 | 0.048 | AMed side |
| AMed/Wrought | 976 | 0.074 | Wrought side |

**Table 6** Chemical compositions of Ti-6Al-4 V plates measured by ICP (wt.%)

| | Al | V | Fe | O | N |
|---|---|---|---|---|---|
| Wrought | 6.39 | 4.17 | 0.21 | 0.16 | 0.006 |
| AMed | 6.23 | 3.97 | 0.07 | 0.11 | 0.026 |
| JIS | 5.50–6.75 | 3.50–4.50 | ≤0.40 | ≤0.20 | ≤0.05 |

Chemical compositions in wrought and AMed Ti6Al4V plates were examined by inductively coupled plasma (ICP) measurement to discuss the different joint characteristics of laser weld AMed/AMed plates and wrought/wrought ones. It is known that oxygen of Ti alloy will lead to reduction of mechanical properties. Nitrogen leads to increase of strength. Carbon also leads to the increase of strength, and the decrease of toughness. As shown in Table 6, there is no significant difference in chemical compositions of wrought and AMed plates. These results suggest that the chemical composition does not affect the difference of tensile strength between AMed/AMed plates and wrought/wrought ones. On the other hand, α' martensite is generated on the AMed plates due to rapid cooling during laser irradiation. Therefore, it is considered that the difference of microstructure for wrought and AMed plates leads to the difference of mechanical properties.

On the other hand, stress–strain curves for weld joint of AMed/wrought plates are shown in Fig. 9c. The laser weld AMed/wrought plates are fractured at wrought base material, and ductile fracture is observed at fracture point. Furthermore, the laser weld joint of AMed/wrought plates shows relatively lower tensile strength and smaller elongation than that of AMed/AMed plates or wrought/wrought plates. The joint characteristics of AMed/wrought Ti6Al4V plates are different from the joint characteristics of AMed/AMed plates or wrought/wrought plates.

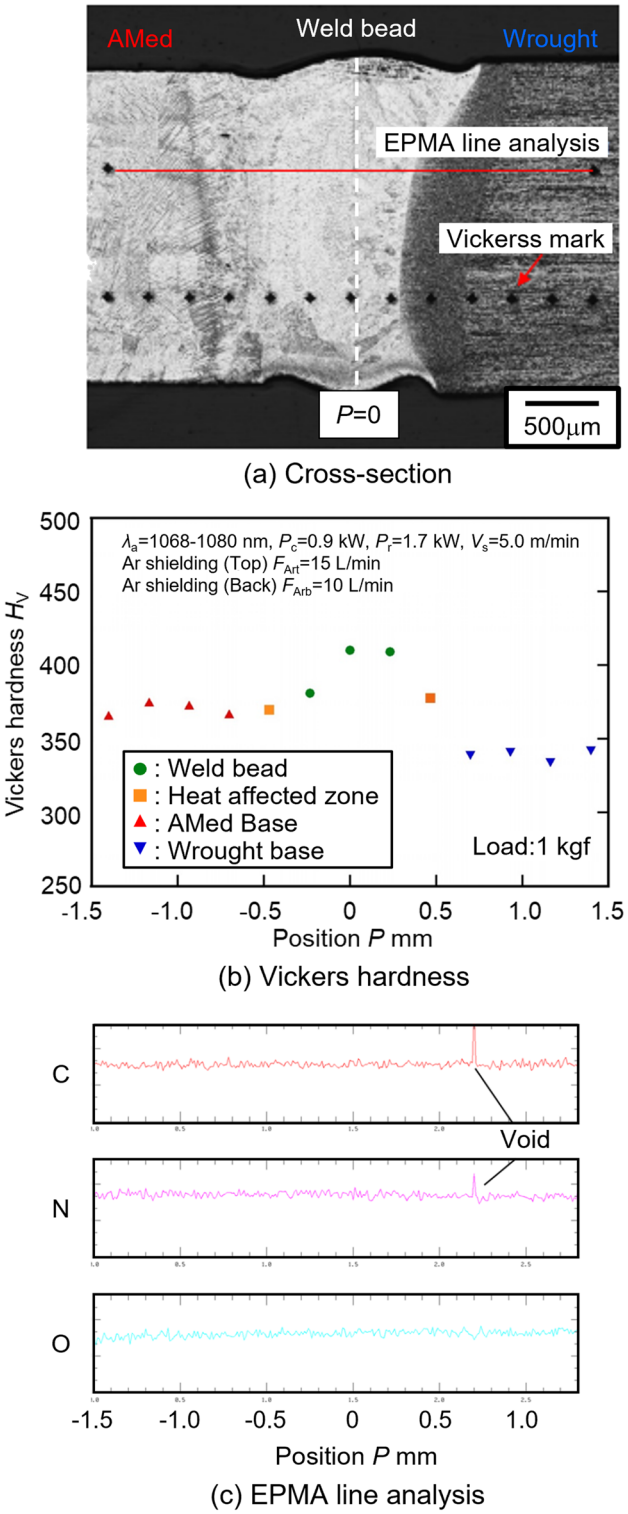


**Fig. 10** Vickers hardness distributions and EPMA line analysis around weld bead

In order to discuss the joint characteristics of AMed/wrought plates, Vickers hardness of weld bead was measured. Cross-section of weld bead of AMed/wrought plates with 2 mm thickness is shown in Fig. 10a. Here, the preparation of specimen for the measurement of Vickers hardness was difficult in the case of 1 mm thickness, and the specimen of 2 mm thickness was used. The laser input power was changed by the specimen thickness, and the heat affected area was different in 1 mm and 2 mm thickness of specimen. However, it is considered that the Vickers hardness distribution around the weld bead would become same tendency between different specimen thickness of 1 mm and 2 mm. The Vickers hardness distribution around the weld bead is shown in Fig. 9b. The Vickers hardness of weld bead is higher than that of other parts. In addition, the hardness of wrought base material is lower than that of AMed one. On the other hand, variations of chemical compositions of carbon, oxygen, and nitrogen at the weld bead were investigated by line analysis of electron probe microanalyzer (EPMA) as shown in Fig. 10c. There is no variation of carbon, oxygen, and nitrogen in AMed base material, weld bead, and wrought base material.

Therefore, good welding state can be confirmed on the weld joint of AMed/wrought plates, since small weld bead with higher hardness is formed between wrought and AMed plates. In addition, fracture at wrought base material is caused by larger elongation and lower tensile strength and lower hardness of wrought base material than AMed base one. The experimental results obtained in this work highlight the different behavior and performance of the material obtained by additive manufacturing from the wrought one, and how this difference affects the characteristics of laser-welded joints, in different combinations of base materials.

## 4 Conclusions

In this study, joint characteristics in laser butt welding of wrought/wrought, AMed/AMed, and AMed/wrought Ti6Al4V plates by fiber laser beam with double core in argon shielding were experimentally investigated. Main conclusions obtained in this study are as follows,

(1) AMed Ti6Al4V plate has higher tensile strength than wrought plate, but elongation of AMed plate is smaller than wrought plate. The different behavior

is attributed to the presence of α' martensitic phase originated for the rapid cooling during laser irradiation in AM process.

(2) Laser weld joint of AMed/AMed plates has higher tensile strength, but smaller elongation than that of wrought/wrought plates.

(3) Laser weld joint of AMed/wrought plates shows that the fracture occurs at the wrought base material because wrought base material has larger elongation and lower tensile strength and lower hardness than AMed base one.

**Funding** Open access funding provided by Okayama University. This research was partly supported by the National Research Foundation (NRF) South Africa Grant No. 118893, and Japan Society for the Promotion of Science (JSPS) JSBP 120196504.

**Data availability** Not applicable.

## Declarations

**Conflict of interest** The authors declare no competing interests.



## References

1. Schmidt M, Merklein M, Bourell D, Dimitrov D, Hausotte T, Wegener K, Overmeyer L, Vollertsen F, Levy GN (2017) Laser based additive manufacturing in industry and academia. CIRP Ann 66:561–583
2. Guddati S, Kiran ASK, Leavy M, Ramakrishna S (2019) Recent advancements in additive manufacturing technologies for porous material applications. Int J Adv Manuf Technol 105:193–215
3. Govekar E, Jeromen A, Kuznetsov A, Levy G, Fujishima M (2018) Study of an annular laser beam based axially-fed powder cladding process. CIRP Ann 67:241–244
4. Yan R, Luo D, Huang H, Li R, Yu N, Liu C, Hu M, Rong Q (2018) Electron beam melting in the fabrication of three-dimensional mesh titanium mandibular prosthesis scaffold. Sci Rep 8:750
5. Szafrańska A, Antolak-Dudka A, Baranowski P, Bogusz P, Zasada D, Małachowski J, Czujko T (2019) Identification of mechanical properties for titanium alloy Ti-6Al-4V produced using LENS Technology. Materials 12:886
6. Izadi M, Farzaneh A, Mohammed M, Gibson I, Rolfe B (2020) A review of laser engineered net shaping (LENS) build and process parameters of metallic parts. Rapid Prototyp J 26(6):1059–1078
7. Squillace A, Prisco U, Ciliberto S, Astarita A (2012) Effect of welding parameters on morphology and mechanical properties of Ti–6Al–4V laser beam welded butt joints. J Mater Process Technol 212:427